

Position sensitive x-ray spectrophotometer using microwave kinetic inductance detectors

Benjamin A. Mazin,^{a)} Bruce Bumble, and Peter K. Day
*Jet Propulsion Laboratory, California Institute of Technology, 4800 Oak Grove Drive, MS 169-506,
 Pasadena, California 91109-8099*

Megan E. Eckart, Sunil Golwala, Jonas Zmuidzinas, and Fiona A. Harrison
*Physics Department, California Institute of Technology, 1200 E. California Blvd., Pasadena, California
 91125*

(Received 30 August 2006; accepted 5 October 2006; published online 29 November 2006)

The surface impedance of a superconductor changes when energy is absorbed and Cooper pairs are broken to produce single electron (quasiparticle) excitations. This change may be sensitively measured using a thin-film resonant circuit called a microwave kinetic inductance detector (MKID). The practical application of MKIDs for photon detection requires a method of efficiently coupling the photon energy to the MKID. The authors present results on position sensitive x-ray detectors made by using two aluminum MKIDs on either side of a tantalum photon absorber strip. Diffusion constants, recombination times, and energy resolution are reported. MKIDs can easily be scaled into large arrays. © 2006 American Institute of Physics. [DOI: 10.1063/1.2390664]

Low temperature detectors (LTDs) are the detectors of choice to measure the energy and arrival time of incoming single photons. Arrays of LTDs can determine the location, time, and energy of every incoming photon (imaging spectrophotometry) with no read noise or dark current. Many technologies are being developed, including doped semiconductor,¹ superconducting tunnel junctions (STJs),²⁻⁴ transition edge sensors (TESs),^{5,6} magnetic microcalorimeters,⁷ and normal-insulator-superconductor bolometers.⁸ While these technologies have shown promise in single pixel and small array devices, multiplexed readouts remain a significant challenge and have only been demonstrated for TES detectors, using complex superconducting circuitry at 4 K (or colder).^{9,10}

The uses of energy-resolving x-ray detectors are both practical and exotic. High resolution x-ray detectors are used in x-ray microanalysis to investigate semiconductor fabrication problems,¹¹ but could also be used to learn about the strong gravitational fields around supermassive black holes. The work described here can also be adapted to optical/UV energy-resolved single photon detection by increasing the responsivity of the detectors. Imaging optical spectrophotometers have a variety of astronomical applications, including planet detection, optical pulsars,¹² and redshift determination of high-*z* galaxies.¹³

An energy-resolving detector for photon energies of 0.1–10 keV can be made using a “strip-detector architecture” (Fig. 1), comprising of a long strip of a superconducting material with quasiparticle sensors attached at each end.² The quasiparticle sensors we use are microwave kinetic inductance detectors¹⁴ (MKIDs), and will be discussed in detail below. STJs have been previously used with this type of detector architecture.²⁻⁴

The photon detection process begins when an x-ray with energy $h\nu$ is absorbed in a tantalum strip, producing a number of excitations, called quasiparticles, equal to $N_{qp} = \eta h\nu / \Delta$, where Δ is the gap parameter of the superconductor and η is an efficiency factor¹⁵ (about 0.6 for our de-

vices). The principle is similar to electron-hole generation by photons in semiconducting x-ray detectors, with the difference that Δ is only tenths of meV, as opposed to 1 eV or more for a semiconductor. This very low gap energy means that millions of quasiparticle excitations are created for each x-ray photon absorbed. Since some of the energy is lost to phonons, the fundamental energy resolution of the detector is limited by the statistical fluctuation of the number of remaining quasiparticles, given by $\sigma_N = \sqrt{FN_{qp}}$, where F is the Fano factor.¹⁶

The tantalum absorber strip has a higher superconducting energy gap ($\Delta=0.67$ meV) than the aluminum MKIDs

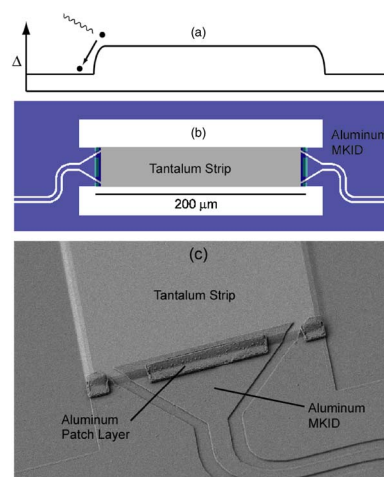


FIG. 1. (Color online) Top panel (a) shows the superconducting gap Δ of the structure, including a quasiparticle diffusing into the aluminum MKID and being trapped by phonon emission. Middle panel (b) contains a drawing of the central region of a MKID strip detector. A $200 \times 35 \mu\text{m}$, 600 nm thick tantalum strip [residual resistivity ratio (RRR)=22.6] is fabricated on *R*-plane sapphire and has MKIDs attached to both ends. The $3 \mu\text{m}$ center strip of the 200 nm thick aluminum (RRR=9.5) CPW resonator that composes the MKID is flared out where it contacts the tantalum strip to allow lateral trapping of quasiparticles. Bottom panel (c) shows a scanning electron microscopy of the Al-Ta interface from the wafer tested in this letter. A patch of aluminum patterned with a lift-off process is used to bridge the Al-Ta interface to avert a step coverage problem. In this device the tantalum is nicely sloped and the aluminum resonator climbs smoothly over the step.

^{a)}Electronic mail: benjamin.mazin@jpl.nasa.gov

($\Delta=0.18$ meV). The quasiparticles created by photons absorbed in the tantalum strip may diffuse laterally, reaching the MKIDs at the two ends of the strip. Once in the MKIDs, the quasiparticles quickly cool by phonon emission. This energy loss prevents them from returning to the higher gap tantalum absorber, trapping them in the MKID. This trapped quasiparticle population is measured by the MKIDs. The two MKID output signals may be used to simultaneously deduce the position and energy of the event. Noise sources will produce some scatter δE in the energy and δx in position; the fractional resolutions in energy and position are expected to be comparable.

The quasiparticles trapped in the MKIDs are sensed through their effect on the kinetic inductance and surface resistance of the aluminum film composing the MKID. The MKIDs are microwave resonators made using coplanar waveguide (CPW) transmission lines.¹⁴ The 3 μm wide CPW center strip is separated from the ground plane by slots that are 2 μm wide. The length of the resonator is ~ 5 mm and the thickness of the Al film is 200 nm. An increase in the quasiparticle population in the MKID moves the resonance frequency lower and increases the width of the resonance (lower quality factor Q). Both of these effects are monitored by measuring the amplitude and phase of a microwave probe signal.¹⁴

The device shown in Fig. 1 was cooled to 150 mK using an Oxford Kelvinox 25 at the Caltech MKID test facility.¹⁷ The test sample contained eight separate strip detectors, with strip lengths of 100, 200, 400, and 800 μm and strip width of 35 μm , and four additional test resonators. For each strip length, two different MKID designs were used, differing in the strength of the coupling to a CPW readout line. The coupling strength is specified by the corresponding coupling-limited quality factor Q_c , which was chosen to be 50 000 and 100 000 for the two MKID designs. All 20 MKID resonators were coupled to a single feed line: the two resonators for a given strip were separated by 20 MHz in frequency, beginning at 6.5 GHz, while a 100 MHz spacing was used to separate the different strip detectors. All the resonators were detected near their design frequencies.

Fabrication of this device is done on an R -plane sapphire wafer to allow epitaxial growth of α -phase (bcc) tantalum. All metal depositions are carried out in a load-locked ultra-high vacuum sputtering system with a base pressure of 10^{-7} Pa. The Ta film is deposited at 60 nm/min to a thickness of 600 nm with substrate temperature of 700 $^\circ\text{C}$. Our layers are patterned using a Canon 3000 stepping mask aligner with a Cymer 250 nm laser. The tantalum film is reactive ion etched (RIE). Tantalum edge sloping is accomplished by reflowing the resist for 5 min at 130 $^\circ\text{C}$, followed by RIE using a gas mixture of 30% O_2 in CF_4 at a pressure of 27 Pa. The resist is eroded back as the tantalum is removed. After the surface is solvent cleaned, it is argon ion cleaned *in situ* before the aluminum for the MKID is blanket deposited to a thickness of 200 nm. RIE of aluminum is done with a mixture of 2:1 $\text{BCl}_3:\text{Cl}_2$ at a pressure of 4 Pa. A water rinse to remove chlorine compounds is followed by a solvent clean.

The device was illuminated with a weak ^{55}Fe source that emits Mn x-rays at $K_\alpha=5.9$ and $K_\beta=6.4$ keV. In order to collect x-ray data we first determine the resonant frequency of the MKIDs from a frequency sweep. Two microwave synthesizers are then used to simultaneously excite and monitor

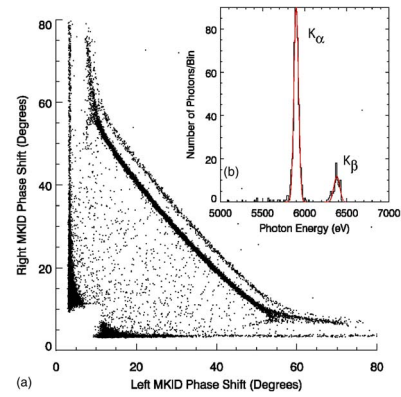


FIG. 2. (Color online) Optimally filtered maximum phase pulse height in degrees observed in aluminum MKIDs attached to a 200 μm tantalum strip is shown in (a). The pulse height in the left MKID is shown on the x axis, while the right MKID is shown on the y axis. The Mn K_α and K_β lines from the ^{55}Fe source are clearly visible. These data are fit to determine the diffusion length, and these are used to compute the energy spectrum shown in the inset (b). We calculate a FWHM energy width $\delta E=62$ eV at 5.899 keV when we restrict our data to all pulses that show greater than 22 $^\circ$ of phase shift in both MKIDs.

the two MKIDs connected to a given strip. X rays absorbed in that strip produce large nearly simultaneous pulses in the phases and amplitudes of the two microwave readout signals. The rise times of the pulses are controlled primarily by the diffusion time in the tantalum strip, while the fall times are set by the quasiparticle lifetime in the aluminum MKIDs. Each of the four readout channels (two MKIDs, the projection of amplitude and phase into rectangular coordinates for each) is sampled at 250 kHz with 16-bit resolution and recorded. A cryoperm magnetic shield surrounds the device.

After data collection we use an optimal filter to determine the maximum pulse height in both channels. This optimal filter is made from a pulse template constructed by averaging many pulses that occur near the center of the strip and using the measured noise spectrum from the MKID. The simplified initial analysis presented in this letter uses only the phase data; however, there is significant information in the amplitude excursion, which we plan to use in a later, more thorough analysis.

These phase pulse data for the 200 μm strip are plotted for both resonators in Fig. 2. We select ten K_α x-ray events with absorption locations spread evenly over the absorber strip. The detailed phase pulse shapes from these events are then used to determine the relevant physical parameters of the device by fitting to a diffusion-recombination model. While each x-ray event is allowed to have a unique absorption location, all ten events are fit using a single set of values for the diffusion constant and quasiparticle lifetime in the tantalum strip and the quasiparticle lifetimes in the two aluminum MKIDs. In addition, a scaling factor accounting for the differing responsivities of the two MKIDs is introduced by allowing a linear prefactor to modify the responsivity of the left MKID. The model also includes a recombination constant (which is the same for both MKIDs) that depends on quasiparticle density in the MKID. This is used to model the enhanced recombination in the aluminum MKID that can occur at the beginning of a pulse if the quasiparticle density is high.

The model starts by placing a Gaussian distribution of quasiparticles with a full width at half maximum (FWHM) of 5 μm in a tantalum strip, which is divided into 200 bins.

TABLE I. Summary of the noise sources present in our resonator. The noise due to quasiparticle creation and recombination (G-R noise) (Ref. 22) in the aluminum MKID is negligible. The intrinsic noise of the device from quasiparticle creation statistics (Fano noise) in tantalum is 2.8 eV. The dielectric in our resonators adds phase noise to the measurement, (Ref. 17), increasing our expected energy width to 65 eV. The excess dielectric noise displayed by this batch of resonators was significantly worse than expected from previous measurements due to the use of a sapphire wafer of poor quality. The best sapphire resonators we have tested which have the dynamic range to measure 6 keV x rays would have given an expected substrate noise contribution of 12 eV.

Noise source	Noise contribution (eV)
G-R noise at 150 mK	0.2
Fano noise in tantalum	2.8
Substrate noise (best)	12
Substrate noise (this device)	65

This initial distribution is propagated forward in time with a time step of 0.1 μs using the Crank-Nicholson method applied to the diffusion equation.¹⁸ At each time step, the number of quasiparticles entering each MKID is recorded. Perfect quasiparticle trapping at the interface is assumed. After the diffusion has been simulated, the quasiparticle pulses are translated into phase pulses using a simple linear model for MKID responsivity, $d\theta/dN_{\text{qp}} = 1.63 \times 10^{-7} \alpha Q/V$ rad per quasiparticle, where $\alpha \approx 0.07$ is the kinetic inductance fraction, $Q \approx 20\,000$ is the resonator quality factor, and V is the volume of the center strip in μm^3 .^{17,19} These simulated pulses are compared with the real data, and an iterative routine is used to find the parameters that best replicate our data. This process is repeated on ten separate sets of pulses in order to produce error estimates.

Using this model we estimate the diffusion and lifetime parameters of the 800 μm long strip since the long length allows the most accurate determination of the material parameters. At a temperature of 150 mK and a microwave readout power at the device of -73 dBm we measure a tantalum diffusion constant of 13.5 ± 1.8 cm^2/s and a tantalum quasiparticle lifetime of 34.5 ± 5.7 μs . The aluminum quasiparticle lifetime is 186 ± 13 μs in the left MKID and 115 ± 8.3 μs in the right MKID. Similar values are obtained from other strips.

These parameters allow us to calculate the tantalum diffusion length $l_{\text{Ta}} = \sqrt{D_{\text{Ta}} \tau_{\text{Ta}}} = 216 \pm 30$ μm and relative responsivity of the MKIDs, which can be used to correct the pulses for quasiparticle loss in the tantalum strip. If we define the loss factor $\beta = l_{\text{strip}}/l_{\text{Ta}}$ using the values from our model, the energy of the photons can be calculated from the pulse heights in each MKID,²⁰ P_1 and P_2 , using $E = \sqrt{P_1^2 + P_2^2 + 2P_1P_2 \cosh(\beta)}$. The inset in Fig. 2 shows the energy histogram derived with this technique for x-ray data taken at 200 mK. When we consider all pulses with greater than 22° of phase shift in each MKID (the center of the absorber strip) we obtain a FWHM energy width $\delta E = 62$ eV at 5.899 keV. This energy width is very close to what we expect from the observed phase noise in the resonators, which predicts an energy width of 65 eV. Table I contains a summary of the noise processes in these detectors.

The responsivity of MKID can be increased by using thinner aluminum films to make the MKID. Thinner films increase the kinetic inductance fraction and decrease the volume, so that film half as thick will have almost four times the

responsivity. For a given maximum photon energy we endeavor to tune the response of the detector to the largest x-ray to about 90° of phase shift. Larger phase excursions involve significant heating of the aluminum film in the MKID and can make the readout and analysis more complex.

If we can reduce our observed noise to the noise we have seen in our best aluminum on sapphire MKIDs with sufficient dynamic range for 6 keV x-rays, we should be able to get an energy resolution of ~ 12 eV, which begins to approach the statistical (Fano) limit in tantalum (3 eV). Further increases in resolution can be expected from a more optimal pulse analysis which includes the amplitude information and from improvements to MKID design and fabrication suggested by our ongoing detailed study of its noise properties.

These strips can easily be stacked into a near 100% fill factor array, and powerful multiplexing techniques to read out large MKID arrays have already been demonstrated.²¹ These strip detectors provide a clear path to large format optical/UV and x-ray focal planes.

The research described in this letter was carried out at the Jet Propulsion Laboratory, California Institute of Technology, under a contract with the National Aeronautics and Space Administration. This work was supported in part by JPL Research and Technology Development funds and by NASA Grant No. NAG5-5322 to one of the authors (F.A.H.). The authors would like to thank Rick LeDuc, Jiansong Gao, Dan Prober, and Luigi Frunzio for useful discussions.

¹C. Stahle, C. Allen, K. Boyce, R. Brekosky, G. Brown, J. Cottam, E. Figueroa-Feliciano, M. Galeazzi, J. Gygax, M. Jacobson, R. Kelley, D. Liu, D. McCammon, R. McClanahan, S. Moseley, F. Porter, L. Rocks, A. Szymkowiak, and J. Vaillancourt, Nucl. Instrum. Methods Phys. Res. A **520**, 466 (2004).

²H. Kraus, T. Peterreins, F. Probst, F. vonFeilitzsch, R. Mossbauer, V. Zacek, and E. Umlauf, Europhys. Lett. **1**, 161 (1986).

³S. Friedrich, K. Segall, M. Gaidis, C. Wilson, D. Prober, A. Szymkowiak, and S. Moseley, Appl. Phys. Lett. **71**, 3901 (1997).

⁴L. Li, L. Frunzio, C. Wilson, and D. Prober, J. Appl. Phys. **93**, 1137 (2003).

⁵K. Irwin, G. Hilton, D. Wollman, and J. Martinis, Appl. Phys. Lett. **69**, 1945 (1996).

⁶B. Cabrera, R. Clarke, P. Colling, A. Miller, S. Nam, and R. Romani, Appl. Phys. Lett. **73**, 735 (1998).

⁷C. Enss, AIP Conf. Proc. **605**, 5 (2002).

⁸D. Schmidt, K. Lehnert, A. Clark, W. Duncan, K. Irwin, N. Miller, and J. Ullom, Appl. Phys. Lett. **86**, 053505 (2005).

⁹J. Chervenak, K. Irwin, E. Grossman, J. Martinis, C. Reintsema, and M. Huber, Appl. Phys. Lett. **74**, 4043 (1999).

¹⁰J. Yoon, J. Clarke, J. Gildemeister, A. Lee, M. Myers, P. Richards, and J. Skidmore, Appl. Phys. Lett. **78**, 371 (2001).

¹¹D. Wollman, K. Irwin, G. Hilton, L. Dulcie, D. Newbury, and J. Martinis, J. Microsc. **188**, 196 (1997).

¹²R. Romani, A. Miller, B. Cabrera, S. Nam, and J. Martinis, Astrophys. J. **563**, 221 (2001).

¹³B. Mazin and R. Brunner, Astron. J. **120**, 2721 (2000).

¹⁴P. Day, H. Leduc, B. Mazin, A. Vayonakis, and J. Zmuidzinas, Nature (London) **425**, 817 (2003).

¹⁵A. G. Kozorezov, A. F. Volkov, J. K. Wigmore, A. Peacock, A. Poelaert, and R. den Hartog, Phys. Rev. B **61**, 11807 (2000).

¹⁶U. Fano, Phys. Rev. **72**, 26 (1947).

¹⁷B. Mazin, Ph.D. thesis, California Institute of Technology, 2004.

¹⁸K. Segall, Ph.D. thesis, Yale University, 2000.

¹⁹J. Gao, J. Zmuidzinas, B. A. Mazin, P. K. Day, and H. G. Leduc, Nucl. Instrum. Methods Phys. Res. A **559**, 585 (2006).

²⁰H. Kraus, F. Vonfeilitzsch, J. Jochum, R. Mossbauer, T. Peterreins, and F. Robst, Phys. Lett. B **231**, 195 (1989).

²¹B. Mazin, P. Day, K. Irwin, C. Reintsema, and J. Zmuidzinas AIP Conf. Proc. **559**, 799 (2006).

²²A. Sergeev and M. Reizer, Int. J. Mod. Phys. B **10**, 635 (1996).